Ordering of mixed paramagnetic and diamagnetic fullerenols in aqueous solutions under magnetic field

V. T. LEBEDEV*, Yu. V. KULVELIS, V. V. RUNOV, V. P. SEDOV, A. A. SZHOGINA
Petersburg Nuclear Physics Institute, NRC Kurchatov Instutute, 188300 Gatchina, Leningrad distr., Russia

Mixtures of paramagnetic $Gd@C_{82}(OH)_X$ and diamagnetic $C_{82}(OH)_X$ (X ~ 30) fullerenols in water have been studied by polarized neutrons at the concentrations C = 0.04 – 2 % wt. At ambient temperature the concentration increase and magnetic field B = 0.001 – 1.0 Tesla strengthening has initiated a growth of molecular correlations at the scale R_C ~15-20 nm, when the aggregation number achieved very high magnitudes ~ $5 \cdot 10^4$ while rather small contribution of nuclear-magnetic interference (≤ 0.1 %) to the total scattering cross section was detected. Thus, in these systems a molecular self-assembly has dominated. This molecular ordering under magnetic field seems to be crucial for their ability to provide a high contrast in medical MRI-diagnostics.

(Received May 7, 2015; accepted June 24, 2015)

Keywords: Fullerenes, Small angle neutron scattering, Structure, Solutions

1. Introduction

A productive controlled synthesis of endofullerenes with metal atoms (EMF) is not achieved till now and EMFs remain still rare substances poorly studied. Nevertheless, the EMFs and their water-soluble forms (fullerenols) promise really good opportunities for numerous advanced applications in biomedicine: isotopic tracers for diagnostics, neuroprotective agents for targeted delivery of drugs inhibiting enzymes, viruses, bacteria; agents for magnetic resonance imaging (MRI), photodynamic therapy [1-3].

For medical applications the hydrated fullerenes (fullerenols) are very attractive as non-toxic, non-immunogenic and non-allergenic substances [4]. These derivatives can be prepared in the reaction of EMFs with NaOH [5]. However in aqueous media the EMFs tend to form molecular aggregates even at low concentrations, and the problem of obtaining highly soluble fullerenols still remains important [5].

The EMFs' functional properties such as contrast effect in MRI are strongly dependent on their molecular assembly in liquid phase (e.g. blood, lymph) [1,2]. A solubility of fullerenols is determined by a number of hydroxyl groups and their arrangement on carbon cages. Therefore a search for the ways of fullerenols' synthesis continues to produce regular structures with a given numbers of OH-groups.

For example, there were obtained amphiphilic molecules $C_{60}(OH)_8$ with regular structure which form stable spherical aggregates in water [6]. In general many of subtle features of fullerenols' aggregation in solution are not clear. It was proposed a concept of association of fullerenols $C_{60}(OH)_{36}$ into the clusters (6-8 nm diameter) with magic numbers of molecules (like metals condensation from gas phase)[7], and the conditions of the growth of such clusters were found. Oppositely to fullerenols $C_{60}(OH)_{36}$, it was not observed a formation of magic clusters for $C_{60}(OH)_{10}$[7].

Preferably the researches of fullerenols concern the derivatives of empty fullerenes, meanwhile the fullerenols of EMF are poorly studied. Recently the authors [8] synthesized and characterized metallofullerenols $Li@C_{60}(OH)_{18}$. The intrinsic electronic structure of $Li^+@C_{60}(O^-)(OH)_n$ defines fullerenols' anionic behavior in solutions (dimethyl sulfoxide, aqueous mixtures) when a repulsion of negatively charged molecules reduces their aggregation as compared with that for empty molecules $C_{60}(OH)_{18}$.

Along with it is much more unstudied the behavior of paramagnetic fullerenols in solutions under magnetic field, although fullerenols' field-induced self-assembly is of great importance for EMF's application as contrast agents for MRI. Recently the authors started such investigation [9].

The present work is devoted to polarized neutron study of self-organization of paramagnetic fullerenols $Gd@C_{82}(OH)_X$ (X~30) mixed with diamagnetic molecules $C_{82}(OH)_X$ when the total content of carbon component is growing and the system approaches to a threshold of solubility in magnetic field.

2. Experimental

The hydroxymetallofullerenes $Gd@C_{82}(OH)_X$ (X = 24-30) and empty fullerenols $C_{82}(OH)_X$ synthesized at PNPI by the original technology including the evaporation of pure carbon rods and the composites with metal compounds in electric arc in helium atmosphere, following extraction and the separation of fullerenes (EMF) and finally their hydroxylation [10,11]. Then the mixtures of hydroxylated metallofullerenes $Gd@C_{82}(OH)_X$ (X = 24-30) and empty fullerenols $C_{82}(OH)_X$ keeping a constant percentage of endohedral structures (30 % wt.)

were prepared and dissolved in light water to have the solutions with concentrations C_1 = 0.044 g/dl, C_2 = 0.56 g/dl, C_3 = 2.0 g /dl covering the range from a dilute system to a system close to the solubility upper limit C_{max} = 2.3 wt.%.

Following experiments on solutions (layer thickness d_S = 1 mm, temperature 20 °C) were carried out on small-angle polarized neutron diffractometer "Vector" (PNPI) in the range of momentum transfer $q = (4\pi/\lambda)\sin(\theta/2)$ = 0.03 - 0.45 nm^{-1} where neutron wavelength λ = 0.92 nm ($\Delta\lambda/\lambda$ = 0.25), scattering angles $0 \le \theta \le 3$ °[12]. The 2D-detector (^{3}He, 300x300 mm^2, efficiency 70%) provided the spatial resolution δ = 1.5 mm along the (X,Y)-coordinates and minimal steps in momentum transfer δq_x, $\delta q_y \approx (2\pi/\lambda)(\delta/L) \approx 4.5\cdot10^{-3}$nm^{-1} for sample-detector base L = 2.3 m. The external field was applied along vertical Y-axis. The incident beam with a vertical polarization ($P_o \approx 0.94$) was oriented horizontally (axis Z).

The scattering from the solutions was isotropic in detector plane even at high magnetic field B = 1.0 Tesla. In following analysis we have used one-dimensional distributions of scattering intensities $I_S(q \equiv q_x)$ corrected for background and the neutron transmissions for the samples. The intensities $I_S(q)$ have been recalculated to get the differential cross section $d\sigma(q)/d\Omega = (I_S/I_W)(d_W/d_S)(d\sigma_W(q)/d\Omega)$ in absolute units (cm^{-1}) per unit solid angle (Ω) and cm^3 of specimen volume. The scattering intensities (I_W) from light water layer (thickness d_W = 1 mm) were measured and the known cross section $d\sigma_W(q)/d\Omega$ = 1.089 cm^{-1} for cm^3 of H_2O (λ = 0.92 nm) was used [13]. Further the cross sections in absolute units are denoted as $\sigma(q) = d\sigma(q)/d\Omega$.

3. Results and discussion

In the experimental q-range (Fig. 1) all the cross sections enhanced at low momentum transfers $q \le 10^{-1}$ nm^{-1} above the incoherent level for light water $\sigma(q) \sim 1$ cm^{-1} at $q \sim 0.5$ nm^{-1}. This indicates a presence of molecular aggregates with characteristic sizes $\ge 10^1$ nm. Moreover the scattering showed a rise roughly proportional to the concentrations C_1 = 0.044 g/dl, C_2 = 0.56 g/dl, C_3 = 2.0 g/dl. This is evidence of the formation of structures with stable aggregation numbers. The influence of magnetic field, B = 0.001; 0.6; 1.0 Tesla, is rather moderate even at high concentration (Fig. 1). The difference between the cross sections $\Delta\sigma(q) = \sigma(q, B) - \sigma(q, B_{min})$ at high and low inductions (B = 1.0 Tesla, B_{min} = 0.001 Tesla) displayed a concentration dependent effect (figure 2). At the lowest concentration (C_1) we found a negative difference $\Delta\sigma(q) < 0$. It reflects scattering weakening at $q \le 10^{-1}$ nm^{-1} in strong field (Fig. 1). It seems doubtful that magnetic field may destroy aggregates and reduce a scattering from specimen respectively. More really the field makes aggregation at larger scale when the scattering concentrates at lower momentum transfers.

On the other hand, in the field B = 1.0 Tesla at moderate and high concentrations (C_2, C_3) the differences $\Delta\sigma(q) > 0$ demonstrate strengthening molecular correlations at the scale $1/q \ge 10^1$ nm (Fig. 2). Overall the concentrations the field-induced variations of cross sections are significant,

$$[\sigma(q,B)-\sigma(q,B_{min})]/\sigma(q,B_{min}) \le 40\%,$$

in spite of low amount of paramagnetic atoms $N = 5\times10^{16}$ - 2×10^{18} cm^{-3} in these systems.

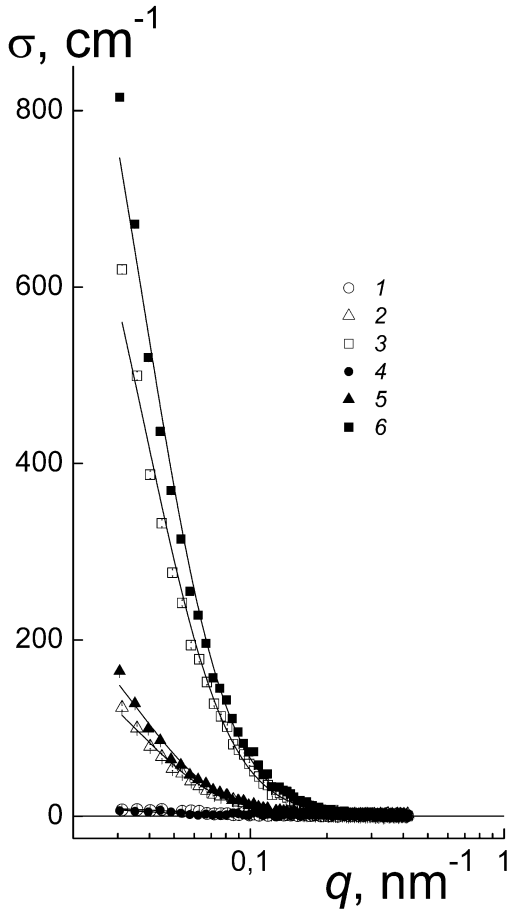

Fig. 1. Cross sections of solutions vs. momentum transfer at fullerenols' concentrations C = 0.044, 0.56 and 2.0 g/dl and magnetic field applied: B = 0.001 (1-3) and 1.0 Tesla (4-6).

Thus, the difference $\Delta\sigma(q) = \sigma(q,B)-\sigma(q, B_{min})$ changes the sign and increases by the transition from highly diluted (C_1) to concentrated system (C_2, C_3) (Fig. 2). The behaviors of the cross sections reflect the evolution of supramolecular structures by changing the concentration and the external field. A molecule of fullerenol can be considered as a spherical particle (diameter d_F ~1.3 nm) having electric and magnetic dipole moments, $P_E \sim 4D$ and $P_M \sim 8\mu_B$ where μ_B is Bohr magneton [14].

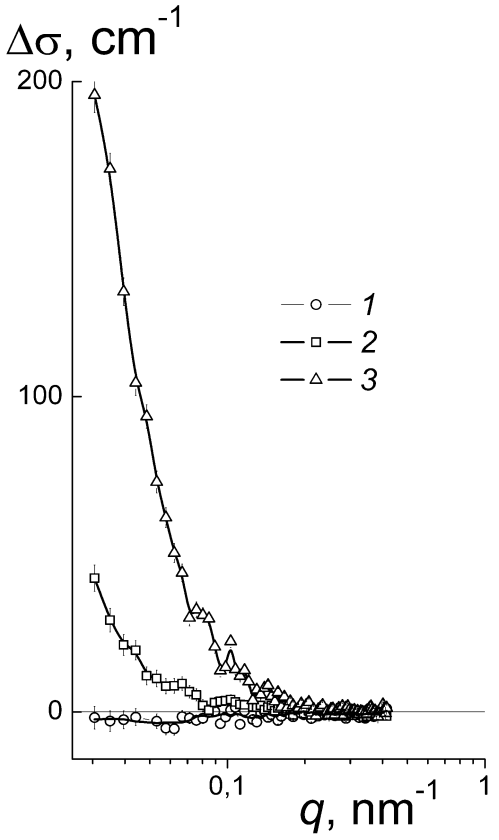

Fig. 2. Difference between the cross sections $\Delta\sigma(q) = \sigma(q,B) - \sigma(q, B_{min})$ in strong and weak fields (B = 1.0 Tesla, B = 0.001 Tesla) vs. momentum transfer for solutions with concentrations: 0.044; 0.56 and 2.0 g/dl (1-3).

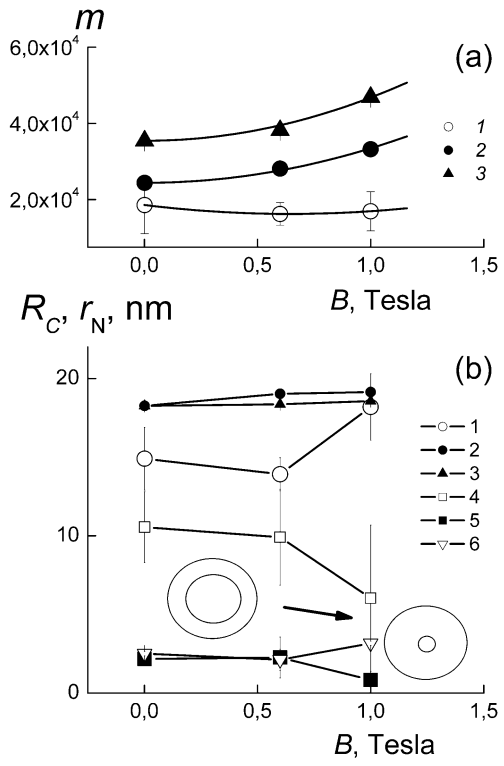

Fig. 3. Parameters of molecular aggregates vs. induction: aggregation numbers m(B,C) (a), correlation radii $R_C(B,C)$ (b) at the concentrations 0.044; 0.56 and 2.0 g/dl (1-3); dense core radii $r_N(B,C)$ inside aggregates at these concentrations (data 4-6). In dilute solution (0.044 g/dl) a field-induced transformation of aggregate with large core (radius r_N) into a particle with small core and characteristic size R_C is shown.

At ambient temperature (T ~ 300 K), if fullerenols contact, the energies of pair dipole interaction normalized to the energy of thermal motion are small, $E_e/k_BT \sim P_E^2/(\varepsilon d_F^3 k_BT) \sim 10^{-3}$, $E_m/k_BT \sim P_M^2/(d_F^3 k_BT) \sim 10^{-6}$. Hence, these interactions are not sufficient for molecular aggregation which can be attributed to hydrogen bonds between the OH-groups of fullerenols and hydrophobic interactions of carbon cages not completely covered with OH-groups. External magnetic field may enhance the interaction of molecules within aggregates and the interaction between them. In following treatment the size of aggregates (correlation radius R_C) and aggregation numbers (m) were found from the q-dependences of cross sections obey the scattering law (Fig. 1)

$$\sigma(q) = \sigma_o[1+ (qR_C)^2]^{-2} + Bg \qquad (1)$$

where σ_0 is the forward cross section and the term Bg shows the contribution of incoherent background. The evaluated parameter $\sigma_0 = (\Delta K)^2\varphi(V_F\ m)$ includes the volume fraction φ of fullerenols, the contrast factor $\Delta K = 4.8\cdot10^{10}$ cm^{-2} and the volume $V_F = 1.2$ nm^3 of a molecule. Finally the aggregation number m was evaluated using the magnitudes of cross section σ_0 and mentioned coefficients (Fig. 3a).

In weak field the diluted system (C_1) has demonstrated the aggregation number $m \sim 2\cdot10^4$ which remains at this level even in strong field while the size of aggregates increases, $R_C \sim 15$ nm $\rightarrow R_C \sim 18$ nm. Hence the aggregates undergo expanding and a conversion into less dense formations. Stronger structuring under field action is observed at higher concentrations C_2 and C_3. The latter is close to the limit of solubility of fullerenols. Initially in low field B = 0.001 Tesla, the aggregation degree at such concentrations achieved the values $m \sim 3\times10^4$ and 4×10^4. In the field B = 1.0 Tesla the degree of aggregation has increased additionally by 30-40% (Fig. 3a) without any enlargement of aggregates, $R_C \approx$ 18-19 nm $\approx$ const, i.e. these structures became denser.

We may conclude that the common feature of the solutions in strong field is a dominance of aggregates of dimension $R_C \approx$ 18-19 nm regardless of the concentration although the aggregation numbers are substantially different in diluted and concentrated systems (C_1, C_3) (Fig.3b). Further the structural features of fullerenols' ensembles were analyzed in terms of correlation functions

$$\gamma(R) = (\Delta K V_F)^2 <\Delta n(0)\Delta n(R)> =$$

$$= (1/2\pi)^3 \int\sigma(q)[\sin(qR)/(qR)]4\pi q^2 dq\ . \qquad (2)$$

The deviations of numerical molecular concentrations (Δn (0), Δn (R)) from a middle level in two points with spacing R define the function $\gamma(R)$. Then we used the functions of pair correlations $G(R) = R^2\gamma(R)$ in spherical presentation and normalized to the concentrations, $G(R)/C$. In figure 4 these are plotted for dilute and more concentrated solutions (C_1, C_2). At higher concentration (C_3) the behavior of correlations is practically the same as when $C = C_2$.

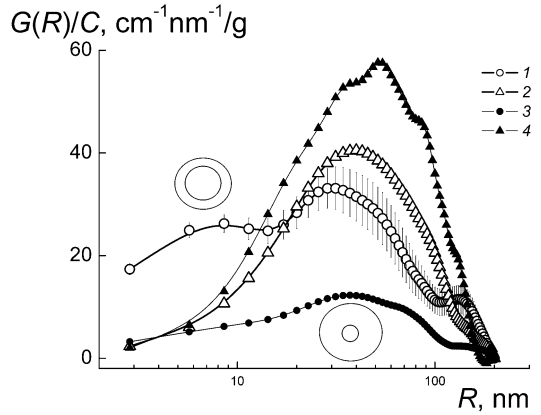

Fig.4. Correlation functions G(R)/C normalized to concentration vs. radius R for solutions with concentrations C = 0.044 (1,3) and 0.56 g /dl (2,4) and the inductions B = 0.001 (1,2) and 1.0 Tesla (3,4). For diluted system when the field becomes strong it is shown the transformation of an aggregate with large dense core into a particle with small core and extended shell.

For diluted system (C_1) in a weak field (B = 0.001 Tesla) the spectrum $G(R)$ shows two maxima at R_1 ~ 10 nm and R_2 ~ 30 nm (Fig. 4). These peaks reflect the internal structure of aggregates which appeared via original molecular self-assembly which was not disturbed in a weak field. In spectrum at low distances around R_1 ~ 10 nm a compact central core inside an aggregate is revealed. More extended correlations related to the second peak at R_2 ~ 30-40 nm ~ $2R_C$ are inherent to rare shell around the core (Fig. 3b). The correlations at the scale $R \geq R_C$ are described by the function $G_C(R) \sim R^2\exp(-R/R_C)$ corresponding to the scattering law (1). The function $G(R)$ reaches a maximum at $R = 2R_C$ and describes the data only in the first approximation when subtle structural details (first peak) are ignored (Fig. 4, data 1). In higher fields B = 0.6 Tesla and B = 1.0 Tesla the first peak disappears, whereas the second peak shifts towards larger radii, R_2 ~ 40 nm. As above its position R_2 ~ 30-40 nm ~ $2R_C$ indicates a double radius of correlations (Fig. 3b). These spectral peculiarities reveal an expansion of the peripheral layers of core when a shell around becomes larger, while the mass of an aggregate do not undergo any substantial changes. On the other hand, at higher content of fullerenols (C_2, C_3), a strong field does not change substantially the size of core and correlation radius of aggregate. However, its mass becomes greater (Fig. 3).

As we established, at moderate and high content of fullerenols (C_2, C_3) a central core in aggregates is not revealed in spectra $G(R)$, since in the total correlations its contribution is masked by the correlations in massive shells. These correlations demonstrate a growth with the induction increase (Fig. 4). This indicates a field-induced amplification of aggregation (Fig. 3a, data 2,3). The proposed model of aggregates with dense core and rare shell is confirmed also by the data analysis using Porod-presentation. The modified cross sections showed the asymptotic behavior at high momentum transfers $\sigma(q)\cdot q^4 \rightarrow I_P = 2\pi(\Delta K_C)^2 S_t$. Thus, the aggregates have a sharp interface between the cores and surrounding shells. In the first approximation the contrast factor is given by $\Delta K_C \approx \Delta K\cdot\varphi_C$ where φ_C is the volume content of fullerenols inside a core. The parameter I_P is proportional to the total area of the borders $S_t = I_P/2\pi(\Delta K_C)^2$ in solution per cm^3. In the calculations of S_t we used the maximum φ_C = 0.74 for the most dense packing of spheres. In spherical approximation we computed the areas of the borders

$$S_t = (C\cdot N_A/mM_F)4\pi r_N^2$$

and the radii of cores

$$r_N = [S_t/(4\pi C\cdot N_A/mM_F)]^{1/2}$$

where N_A is Avogadro constant, M_F is the mass of a fullerenol (Fig. 3b, data 4-6). These calculations for dilute solution (C_1) in weak or moderate field (B = 0.001; 0.6 Tesla) gave the size of core r_N ~ 10 nm ~ 2/3 of the correlation length R_C (Fig. 3b, data 4). In strong field (B = 1.0 Tesla) the core is shrunken, r_N ~ 6 nm ~ (1/3)R_C. While in more concentrated systems (C_2,C_3), a strong magnetic field makes the core radius r_N ~ 2-3 nm much smaller than the length of correlations R_C, and rarefied shells prevail in aggregates (Fig. 3b).

4. Conclusion

Neutron scattering studies of the mixtures of paramagnetic and diamagnetic fullerenols in water at various concentrations of carbon component demonstrated very specific features of magnetic field action on molecular assembly. At high dilution (0.044 g/dl) in weak field (B = 0.001 Tesla), the ensemble of fullerenols displayed a condensation into massive aggregates (~10^4 molecules) with large dense cores and thin shells. However strong external field (B = 1.0 Tesla) altered substantially the original self-organization and facilitated in aggregates a transformation of cores' external layers into gel-like shells around the cores. In a wide range of concentrations (0.044 - 2.0 g/dl) the induction B = 1.0 Tesla is sufficient to convert the aggregates into stable supramolecular structures with correlation radius R_C ~ 20 nm and aggregation numbers $m \geq 10^4$.

These results have demonstrated really stable forms of self-organization of mixed paramagnetic and diamagnetic

fullerenols in aqueous solutions by strong varying concentration and external magnetic field. This should be considered as an important aspect related to potential applications of metallofullerenes in medical diagnostics for a creation of effective contrasts in MRI.

Acknowledgements

The work was supported by RFBR (grant 14-23-01015 ofi_m).

References

[1] J. Grebowski, P. Kazmierska, A. Krokosz, BioMed Research International. Article ID 751913, 9 pages http://dx.doi.org/10.1155/2013/751913 (2013).
[2] M.Carini, L. Dordevic, T. Da Ros. Fullerenes in Biology and Medicine. Handbook of Carbon Nanostructures. Vol. 3, Ch.1, 344 pp. (2013).
[3] K. Kokubo, Water-soluble Single Nano Carbon Particles: Fullerenols and Its Derivatives. The delivery of Nanoparticles. Dr. Abbass A Hashim (Ed.) ISBN: 978-953-51-0615-9 In Tech http:/www.intechopen.com/books (2012).
[4] G. V. Andrievsky, V. I. Bruskov, A .Tykhomirov, S. V. Gudkov, Free Radical Biology & Medicine. **47,** 786 (2009).
[5] X. Li, Z. Chen, G. Guo, S. Deng, J. Instrumental Analysis. **28(**4), 432 (2009).
[6] G. Zhang, Y. Liu, D. Liang, L. Gan, Y. Li. Angewandte Chemie International Edition. **49(**31), 5293 (2010).
[7] Y. Nakamura, H. Ueno, K. Kokubo, N. Ikuma, T. Oshima J. Nanopart. Res. **15,** 1755 (2013).
[8] H. Ueno, Y. Nakamura, N. Ikuma, K. Kokubo, T. Oshima, Nano Res. **5(**8), 558 (2012).
[9] V. T. Lebedev, Yu. V. Kulvelis, V. V. Runov, V. P. Sedov, A. A. Szhogina, Journal of Surface Investigation. X-ray, Synchrotron and Neutron Techniques, **8,** 5, 1044 (2014).
[10] V. P. Sedov, A. A. Szhogina, Methods of synthesis and identification of hydroxylated fullerenes – fullerenols. Preprint of the Petersburg Nuclear Physics Institute, No 2953, Gatchina, 43 p. (2014) (Rus.).
[11] V. P. Sedov, A. A. Szhogina, Method for producing water-soluble derivatives of fullerenes. Patent submission No 2014113248 / Sedov V.P., Szhogina A.A.; priority from 26.05.14 (2014).
[12] V. V. Runov, Pisma v ZhETF. **95**(9), 530 (2012) (Rus.)
[13] P. Lindner, J. Appl. Cryst. **33(**3), 807 (2000).
[14] V. K. Koltover, Vestnik RFFI. **3**(59), 54 (2008) (Rus).

*Corresponding author: vlebedev@pnpi.spb.ru